Cellular/Molecular

Carbonic Anhydrases CA4 and CA14 Both Enhance AE3-Mediated Cl^-–HCO_3^- Exchange in Hippocampal Neurons

Nataliya Svichar,[1] Abdul Waheed,[2] William S. Sly,[2] Jean C. Hennings,[3] Christian A. Hübner,[3] and Mitchell Chesler[1]

[1]Department of Neurosurgery, New York University Langone Medical Center, New York, New York 10016, [2]Department of Biology and Edward A. Doisy Department of Biochemistry and Molecular Biology, Saint Louis University School of Medicine, St. Louis, Missouri 63104, and [3]Department of Clinical Chemistry, Friedrich-Schiller-Universität, D-07747 Jena, Germany

Carbonic anhydrase (CA) activity in the brain extracellular space is attributable mainly to isoforms CA4 and CA14. In brain, these enzymes have been studied mostly in the context of buffering activity-dependent extracellular pH transients. Yet evidence from others has suggested that CA4 acts in a complex with anion exchangers (AEs) to facilitate Cl^-–HCO_3^- exchange in cotransfected cells. To investigate whether CA4 or CA14 plays such a role in hippocampal neurons, we studied NH_4^+-induced alkalinization of the cytosol, which is mitigated by Cl^- entry and HCO_3^- exit. The NH_4^+-induced alkalinization was enhanced when the extracellular CAs were inhibited by the poorly permeant CA blocker, benzolamide, or by inhibitory antibodies specific for either CA4 or CA14. The NH_4^+-induced alkalinization was also increased with inhibition of anion exchange by 4,4*-diisothiocyanostilbene-2,2*-disulfonic acid, or by eliminating Cl^- from the medium. No effect of benzolamide was seen under these conditions, in which no Cl^-–HCO_3^- exchange was possible. Quantitative PCR on RNA from the neuronal cultures indicated that AE3 was the predominant AE isoform. Single-cell PCR also showed that Slc4a3 (AE3) transcripts were abundant in isolated neurons. In hippocampal neurons dissociated from AE3-null mice, the NH_4^+-induced alkalinization was much larger than that seen in neurons from wild-type mice, suggesting little or no Cl^-–HCO_3^- exchange in the absence of AE3. Benzolamide had no effect on the NH_4^+-induced alkalinization in the AE3 knock-out neurons. Our results indicate that CA4 and CA14 both play important roles in the regulation of intracellular pH in hippocampal neurons, by facilitating AE3-mediated Cl^-–HCO_3^- exchange.

Introduction

Carbonic anhydrase (CA) on the extracellular membrane surface is found in a variety of tissues that include kidney (Wistrand and Knuuttila, 1989; Kaunisto et al., 2002), lung (Waheed et al., 1992a), and skeletal muscle (Waheed et al., 1992b). In the CNS, the presence of extracellular CA (ECA) was detected in physiological studies of rat hippocampal slices, in which a role was established in both the generation (Kaila et al., 1992) and buffering (Chen and Chesler, 1992a,b) of different classes of activity-dependent alkaline extracellular pH (pH_e) shifts. The enzyme was indirectly implicated in regulation of excitatory synaptic transmission, because the curtailment of extracellular alkaline shifts by ECA was shown to limit postsynaptic NMDA receptor activation during synchronous neural activity (Fedirko et al., 2007). The principal isoforms of ECA in the brain are CA4 (Tong et al., 2000; Wang et al., 2002) and CA14 (Parkkila et al., 2001), and both enzymes catalyze the buffering of activity-dependent pH_e transients (Shah et al., 2005).

Although ECA plays a role in buffering the brain extracellular space, the CAs are also involved in the transport of protons or bicarbonate (Breton, 2001; McMurtrie et al., 2004). In heterologous expression systems, surface CA4 was shown to facilitate the Cl^-–HCO_3^- exchangers AE1, AE2, and AE3 (with respective gene names Slc4a1, Slc4a2, and Slc4a3) (Sterling et al., 2002). These carriers serve as acid-loading mechanisms that respond to a rise in cytosolic pH (pH_i) by exchanging intracellular HCO_3^- for external Cl^- (Romero et al., 2004).

This issue is of particular interest with respect to hippocampal neurons, because these cells exhibit robust Cl^-–HCO_3^- exchange activity (Raley-Susman et al., 1993; Brett et al., 2002), have abundant transcripts for AE3 (Kopito et al., 1989; Raley-Susman et al., 1993), and express both CA4 (Wang et al., 2002) and CA14 on cell surfaces (Parkkila et al., 2001). Knock-out of AE3 has been shown to lower the threshold for the generation of seizure in mice, perhaps because of impairment of neuronal pH regulation in hippocampal neurons (Hentschke et al., 2006). In addition, Cl^- transport by AE3 may influence the reversal potential for fast inhibitory synaptic transmission, as was reported in embryonic motoneurons (Gonzalez-Islas et al., 2008).

To address whether ECA facilitates transport by AE3 in hippocampal neurons, we studied the rise in pH_i elicited by brief exposure to NH_4^+. Our data show that acid loading to oppose this alkalosis is facilitated by ECA. In addition, ECA augmented the rate of pH_i recovery from the fall in pH_i that ensued on withdrawal of NH_4^+. Using specific inhibitory antibodies against CA4 and CA14, we demonstrate that both isoforms play a role in opposing intracellular alkaline loads. Using neurons from AE3

Received Dec. 17, 2008; revised Feb. 9, 2009; accepted Feb. 12, 2009.

This work was supported by National Institutes of Health Grant R01 NS032123 and the Attilio and Olympia Ricciardi Fund.

Correspondence should be addressed to Dr. Mitchell Chesler, Department of Neurosurgery, New York University Langone Medical Center, 550 First Avenue, New York, NY 10016. E-mail: mitchell.chesler@nyumc.org.

DOI:10.1523/JNEUROSCI.0036-09.2009

 0270-6474/09/293252-07$15.00/0

knock-out versus wild-type mice, we also show that this effect of ECA on intracellular alkalosis requires the expression of AE3. These results demonstrate that both CA4 and CA14 contribute to neuronal pH regulation by enabling the acid-loading function of AE3. A preliminary report of these findings has appeared previously (Svichar et al., 2007).

Materials and Methods

Hippocampal neuronal cultures. All procedures were performed with approval of the Institutional Animal Care and Use Committee of the New York University School of Medicine. Pregnant Swiss Webster (Taconic) mice [at embryonic day 12 (E12) to E18] were killed by CO_2 narcosis. Embryos were removed under sterile conditions, decapitated, and placed into ice-cold dissecting medium. Eight hippocampi from E18 embryos were minced into 1-mm-thick pieces against the wall of a 50 ml conical tube containing 0.5 ml of 2.5% Trypsin (Invitrogen) and 4.5 ml of L15 medium (Invitrogen). The conical tube was placed in the incubator at 37°C for 15 min, shaking every 5 min. The supernatant was removed into another tube containing 0.5 ml of FBS (Invitrogen) (to inactivate trypsin). The pellet was placed in 4.5 ml of L15 medium with 0.025% deoxyribonucleases (Dnase; Sigma-Aldrich) and incubated for 5 min (37°C), and then L15 media with inactivated trypsin was added. The cells were then concentrated by centrifugation (750 rpm; 5 min), and the supernatant was decanted. Fresh complete culture medium (NBM plus B27 supplement; Invitrogen) was added to resuspend the pellet. The pellet was dissociated by trituration using a pipette tip into a single-cell suspension. Cells were plated onto 22 × 22 mm cover glasses coated with poly-D-lysine (Sigma-Aldrich), inserted into six-well plates, and incubated at 37°C in a 5% CO_2, atmosphere overnight. Complete NBM (1.5 ml) was added to the wells to bring up the volume. Experiments were performed after 14–21 d in culture.

Acutely dissociated hippocampal neurons. Hippocampal neurons from area cornu ammon 1 were dissociated from adult AE3 knock-out and wild-type mice based on the protocol of Mintz et al. (1992). Anesthetized animals were decapitated, the brain excised, and 300 μm hippocampal slices cut and incubated in standard bicarbonate-buffered saline (see below) at room temperature. Slices were then transferred to oxygen-equilibrated dissociation solution containing Sigma-Aldrich type XXIII protease (3 mg/ml) and gently stirred for 27–30 min. at 37°C. After washing off protease, slices were stirred for 7 min in DNase (bovine type IV; 0.5 mg/ml) with trypsin inhibitor (Boehringer Mannheim; 1 mg/ml). The cornu ammon zone 1 of hippocampus was isolated from the slice and mechanically dissociated using glass pipettes of progressively finer bore. Cells were plated onto concanavalin A-coated coverslips and left to settle for 1–2 h before use. Pyramidal neurons were identified morphologically by their large size, pyramidal shape, and distinct basal and apical dendritic arbors (Tse et al., 1992).

Experimental solutions and drugs. Standard bicarbonate-buffered saline contained the following (in mM): 124 NaCl, 26 $NaHCO_3$, 3.0 KCl, 1.0 NaH_2PO_4, 2.0 $CaCl_2$, 1.5 $MgCl_2$, and 10 glucose (95% O_2–5% CO_2, pH 7.4). With addition of 20 mM NH_4^+, the NaCl concentration was dropped to 104 mM. In zero chloride saline, the NaCl, KCl, $CaCl_2$, and $MgCl_2$ were substituted with Na-methanesulfonate, K^+-methanesulfonate, $CaSO_4$, and $MgSO_4$, respectively. With use of 20 mM NH_4^+ in zero Cl^- saline, 20 mM Na-methanesulfonate was replaced by 20 mM ammonium methanesulfonate. Solutions were warmed to 32°C and were superfused at 2 ml/min. During incubations with antisera, the flow was stopped. To avoid large increases in solution pH that could occur because of loss of CO_2 from the static bath, a HEPES-buffered saline was used for the antisera incubations. The HEPES saline contained the following (in mM): 124 NaCl, 3.0 KCl, 1.0 NaH_2PO_4, 2.0 $CaCl_2$, 1.5 $MgCl_2$, 10 glucose, 26 HEPES (titrated to pH 7.4 with NaOH), and was gassed with 100% O_2. 4,4*-Diisothiocyanostilbene-2,2*-disulfonic acid (DIDS) was obtained from Sigma-Aldrich. Benzolamide was a gift from Dr. E. R. Swenson (University of Washington, Seattle, WA).

Recording of intracellular pH. Coverslips with attached astrocytes served as the floor of a submersion chamber mounted on the stage of a Zeiss Axiovert inverted microscope equipped for epifluorescence. Neurons were loaded with the acetoxy-methylester form of the pH-sensitive fluorophore BCECF (2 μM in Ringer's) for 10 min at room temperature. A 75 W xenon lamp and a monochrometer provided alternate 490 and 440 nm fluorescence excitation (Photon Technology International). Emissions >535 nm (F_{440} and F_{490}, respectively) were collected via a 40× oil-immersion objective and an 8 bit intensified CCD camera. Averaged fluorescence from regions of interest around single neurons was imaged at 15 s intervals using ImageMaster software (Photon Technology International). For each experiment, the F_{490}/F_{440} ratio was displayed as simultaneous line traces from multiple neurons. The F_{490}/F_{440} ratio was converted to intracellular pH using the nigericin single-point technique (Boyarsky et al., 1988) that used a HEPES-buffered calibration solution (150 mM K^+ and 3 μM nigericin, pH 7.0) superfused at the end of each experiment. Data were referenced to a calibration curve previously constructed using similar nigericin–150 mM K^+ solutions buffered with PIPES or HEPES over the pH range of 6.0–8.0.

Characterization of inhibitory antibodies against CA4 and CA14. Antibodies against mouse CA4 or mouse CA14 were raised in rabbits inoculated with respective affinity-purified recombinant enzymes (Zhu and Sly, 1990). Antisera and preimmune sera were dialyzed against HEPES-buffered physiological saline. To test the ability of these antisera to inhibit CA activity, 0.5–1.0 EU equivalent of purified recombinant CA4 or CA14 (Parkkila et al., 2001) was incubated with 2 μl of antisera at 37°C for 30 min. Enzyme activity was then quantified using the fish tank procedure of Maren (1960), as described previously (Sundaram et al., 1986). Percentage inhibition was calculated from the average of three independent experiments. Results for antisera to rat CA4, mouse CA4, and mouse CA14 are shown in Table 1. Both antisera caused a pronounced inhibition of the activity of its target protein and had negligible effect in cross-isoform or cross-species testing.

Table 1. Inhibition of CA activities by specific antibodies

	Percentage inhibition of CA activity		
Antibodies	Rat CA4	Mouse CA4	Mouse CA14
Anti-mouse CA4	4 ± 2	88 ± 5	4 ± 2
Anti-mouse CA14	4 ± 2	5 ± 3	89 ± 5

Characterization of inhibitory antibodies against CA4 and CA14. A total of 0.5–1.0 EU equivalent CA isozymes was used. Two microliters of antiserum was incubated at 37°C for 30 min before CA assay. Percentage inhibition was calculated from the average of three independent experiments.

Detection of surface CA activity using inhibitory antisera. In bicarbonate saline, neurons were exposed to 20 mM NH_4^+ for 5 min. After the characteristic sequence of intracellular pH transients (see Results), the flow was stopped, and the coverslip was overlaid with 200 μl of antisera to either CA4, or CA14, or the respective preimmune sera (each diluted as 20 μl of sera in 200 μl of HEPES-buffered saline). After 30 min of incubation, the flow of bicarbonate saline was resumed, and a second exposure to 20 mM NH_4^+ commenced. The amplitudes of the initial rise in pH_i on exposure to NH_4^+ were compared for control and postincubation trials.

RNA extraction, reverse transcription, and PCR. Total RNA from neuronal cultures was isolated using RNeasy mini kit (QIAGEN) and reverse transcribed into a single-stranded cDNA with SuperScript II Reverse Transcriptase kit (Invitrogen) per manufacturer's instructions. The resulting first-strand cDNA was then used as a template for SYBR Green real-time PCR.

Primers were designed with Primer 3.0 (Whitehead Institute for Biomedical Research, Cambridge, MA). The cDNA sequences were obtained from the GenBank database of the National Center for Biotechnology Information. All primer pairs were designed as intron spanning. Primers are listed in Table 2. The amplification efficiency for each individual PCR was calculated from the kinetic curve. The initial amount of gene transcript was derived based on the method of Liu and Saint (2002). Transcript level is presented as the fraction of the target gene transcripts per 1000 transcripts of reference gene (β-actin; gene name, Actb).

For single-cell PCR, the cytoplasm of a neuron was aspirated into the patch pipette filled with a 5× buffer (Promega) containing RNase inhibitor (Eppendorf; 20 U/ml), and then expelled into a microcentrifuge tube

Table 2. Primers used in PCRs

Gene	Accession no.	Fragment	Forward primer	Reverse primer
Real-time PCRs				
Slc4a1	NM_011403	1187–1301	AGCTGCTTAGGAGGCGGTA	CGTAGAGGGTCGTCTTCGTC
Slc4a2	NM_009207	1121–1221	GCATAAGCCCCATGAGGTGT	CCTCGAATTTTATCCAGCGG
Slc4a3	NM_009208	2100–2207	GGAACAGACCAAGGTGGAGA	AGGGGATCGTCTTCAGAGGT
Car4	NM_007607	741–838	CAACCCATCAAGATCCACAA	GGCCTCACATTGTCCTTCAT
Car14	NM_011797	462–578	CCCATGGATATGACCAGCTT	CTGTGTATTTTCGGGGCAGT
Actb	NM_007393	858–911	GCTCTTTTCCAGCCTTCCTT	AGTTTCATGGATGCCACAGG
Multiplex PCRs				
Slc4a3	NM_009208	2879–3635	CGTTCCTCATTGCCTTCTTC	ATCCGCCATGTCTTCACCTT
Actb	NM_007393	305–877	TGTTACCAACTGGGACGACA	AAGGAAGGCTGGAAAAGAGC
Nested PCRs				
Slc4a3	NM_009208	3322–3536	GTGCGCTCTGTCACTCATGT	AGTGATGTGACGCCCATGTA
Actb	NM_007393	470–696	AGCCATGTACGTAGCCATCC	TCTCAGCTGTGGTGGTGAAG

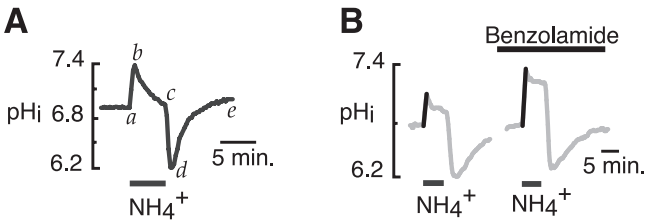

Figure 1. The effect of benzolamide on NH_4^+-induced pH_i transients in cultured mouse hippocampal neurons. ***A***, Example of typical sequence of pH_i transients elicited by a 5 min exposure to 20 mM NH_4^+ (for details, see text). ***B***, Amplification of the NH_4^+-induced alkalinization (NIA) by benzolamide (10 μM in all experiments). The NIA is shown in bold for all figures.

containing the reaction mixture for reverse transcription. The first-strand cDNA was synthesized with ImProm II Reverse Transcriptase (Promega) following manufacturer's instructions. After reverse transcription, the cDNAs for Slc4a3 and β-actin were amplified simultaneously in a multiplex PCR. The final product was diluted 10 times and nested PCR performed for each gene separately. The products of nested PCR were separated and visualized on an ethidium bromide-stained agarose gel.

Data analysis. Data were presented as means with SE. Paired comparisons were conducted using a two-tailed Student *t* test. Comparisons of the rate of pH_i recovery from alkalosis or acidosis were restricted to pairs of control versus treated cells for which there was an overlap of pH_i during the initial linear phase of recovery. Therefore, not all coverslips could be used for comparative data on rates of recovery.

Results

The effect of benzolamide on NH_4^+-induced pH_i transients in hippocampal neurons

Transient exposure of cells to NH_4^+ produces a well established sequence of pH_i shifts (Boron and De Weer, 1976), as illustrated for a cultured hippocampal neuron in Figure 1*A*. A variable initial rise in pH_i occurs because of the entry of NH_3 (Fig. 1, segment *a–b*). This alkaline shift is followed by a slower, variable fall in pH_i (segment *b–c*) because of both the passive entry of NH_4^+ and the passive efflux of bicarbonate by membrane transporters (see below). On withdrawal of NH_4^+ from the bathing media, a sharp fall in pH_i occurs, as the accumulated intracellular NH_4^+ exits in the form of NH_3, leaving behind a cytosolic H^+ load (segment *c–d*). Recovery from this acidification then ensues (segment *d–e*) because of the action of plasma membrane acid extruders (Roos and Boron, 1981; Thomas, 1984).

The amplitude of the initial NH_4^+-induced alkalinization (NIA) was markedly increased in the presence of benzolamide (10 μM), a poorly permeant inhibitor of CA (Fig. 1*B*). The mean NIA amplitudes were 0.39 ± 0.02 versus 0.54 ± 0.02 unit pH, in the absence and presence of benzolamide, respectively ($p < 0.001$; $n = 37$ cells/7 coverslips). Such an increase in NIA amplitude would be expected if benzolamide had suppressed operation of an acid-loading mechanism that normally opposed the alkalosis.

Benzolamide also had significant, but less consistent effects on the rates of recovery from alkalinization and acidification, corresponding to segments *b–c* and *d–e*, respectively, in Figure 1*A*. The mean rate of recovery from alkalosis decreased from 0.18 ± 0.02 before, to 0.12 ± 0.02 unit pH per minute after addition of benzolamide ($n = 19$ cells, 3 coverslips; $p < 0.01$). The rate of recovery from acidosis was also slowed, falling from 0.20 ± 0.04 before, to 0.12 ± 0.02 unit pH per minute after addition of benzolamide (18 cells, 3 coverslips; $p < 0.05$). The effect on the rates of pH_i recovery from alkalosis and acidosis were not noted in all cells studied, but overall suggested that surface CA could facilitate both acid loading that opposed NIA, and acid extrusion responsible for pH_i recovery after withdrawal of NH_4^+. The facilitation of acid extrusion mechanisms and recovery from acidosis by ECA has been noted in other cells, in which it apparently augmented the operation of Na^+–H^+ exchange (Wu et al., 1998), and Na^+–HCO_3^- cotransport (Alvarez et al., 2003). In the present study, however, the most consistent, reproducible effect of benzolamide on NH_4^+-induced pH_i transients was the increase in the NIA.

The roles of CA4 and CA14 in curtailment of the NIA

To test whether either or both surface enzymes were responsible for limiting the amplitude of the NIA, we used specific inhibitory antisera against each isoform. After eliciting a control NIA, neurons were incubated with CA4 antisera for 30 min. After washout of the antisera, a second NIA was elicited. In this paired comparison, the mean control NIA of 0.21 ± 0.04 unit pH was increased to 0.38 ± 0.02 after incubation in CA4 antisera ($p < 0.001$; $n = 12$ cells, 5 coverslips), but was unchanged when cells were incubated in preimmune sera (Fig. 2*B*) (0.35 ± 0.04 vs 0.30 ± 0.06 unit pH; $n = 8$ cells, 4 coverslips; $p = 0.21$).

We similarly tested whether inhibition of CA14 could amplify the NIA. The mean control NIA of 0.20 ± 0.03 unit pH was increased to 0.36 ± 0.03 after incubation in CA14 antisera (Fig. 3*A*) ($p < 0.001$; $n = 14$ cells, 4 coverslips), but was unchanged when cells were incubated in preimmune sera (Fig. 3*B*) (0.21 ± 0.02 vs 0.23 ± 0.02 unit pH; $n = 14$ cells, 4 coverslips; $p = 0.33$). Thus, both isoforms of surface CA played a role in suppressing the NIA.

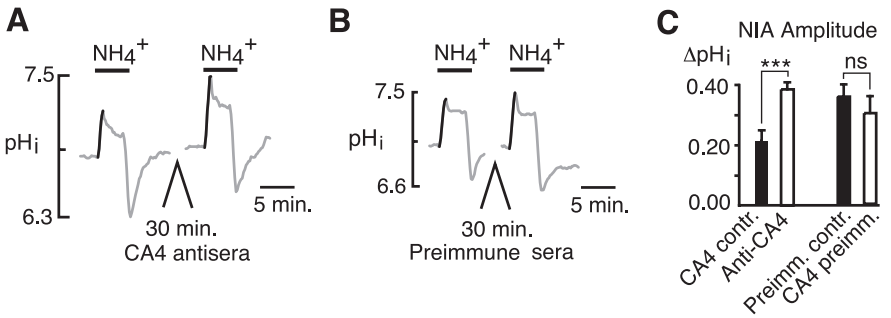

Figure 2. Effect of CA4 inhibitory antisera on the NIA in hippocampal neurons. ***A***, The NIA was significantly increased after a 30 min incubation in CA4 antisera. ***B***, A similar 30 min incubation in preimmune sera had no effect on the NIA. ***C***, Mean amplitudes of the NIA in control (CA4 contr.) versus CA4 antisera incubation (Anti-CA4) and of NIA before (Preimm.contr.) and after (CA4 preimm.) incubation in preimmune sera (paired trials). Statistical measures are given as follows: $^{***}p < 0.001$; $^{ns}p > 0.05$. Error bars indicate SEM.

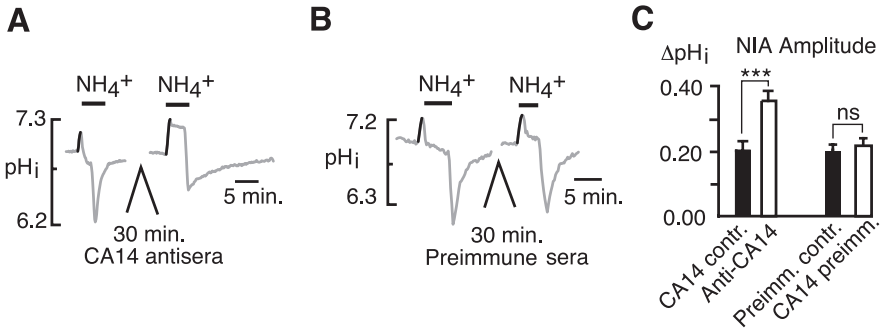

Figure 3. Effect of CA14 inhibitory antisera on the NIA in hippocampal neurons. ***A***, The NIA was significantly increased after a 30 min incubation in CA14 antisera. ***B***, A similar 30 min incubation in preimmune sera had no effect on the NIA. ***C***, Mean amplitudes of the NIA in control (CA14 contr.) versus CA14 antisera (Anti-CA14) and of NIA before and after incubation in preimmune sera (Preimm.contr. and CA14 preimm., respectively) (paired trials). $^{***}p < 0.001$; $^{ns}p > 0.05$. Error bars indicate SEM.

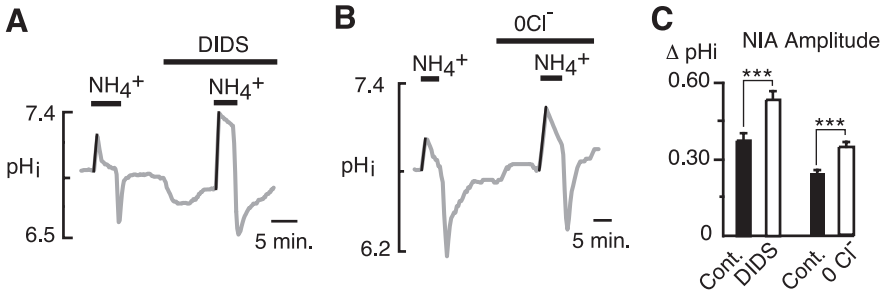

Figure 4. Inhibition of Cl^-–HCO_3^- exchange is associated with an increased NIA. ***A***, The NIA was increased by the stilbene derivative DIDS (100 μM). ***B***, In Cl^--free saline, the NIA was increased. ***C***, Mean amplitudes of the NIA in control versus DIDS, and control versus 0 Cl^- (paired trials). $^{***}p < 0.001$. Error bars indicate SEM.

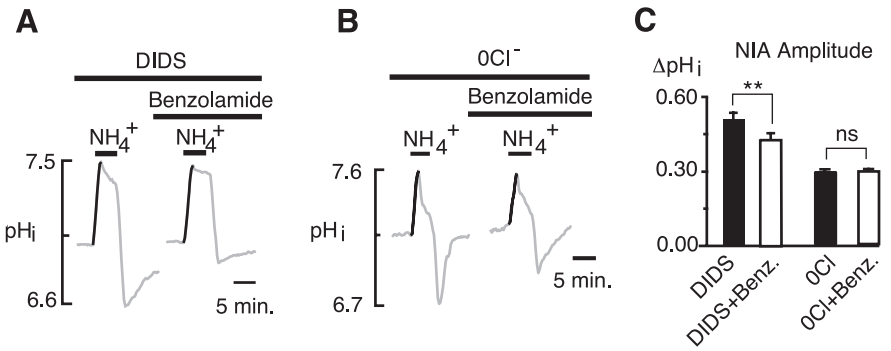

Figure 5. Inhibition of Cl^-–HCO_3^- exchange occluded the effect of benzolamide. ***A***, In the presence of DIDS, the addition of benzolamide did not increase the NIA. ***B***, In Cl^--free saline, the addition of benzolamide did not alter the NIA. ***C***, Mean amplitudes of the NIA in DIDS versus DIDS with benzolamide, and in 0 Cl^- versus 0Cl^- with benzolamide (paired trials). $^{**}p < 0.01$; $^{ns}p > 0.05$. Error bars indicate SEM.

The NIA is curtailed by Cl^-–HCO_3^- exchange

The acid-loading mechanism that typically counters alkalinization of the cytosol is Cl^-–HCO_3^- exchange, which in brain exists principally as the anion exchanger (AE) isoform AE3 (Kopito et al., 1989). If Cl^-–HCO_3^- exchange were responsible for curtailing the NIA, then classic means of inhibiting this mechanism would be expected to result in a larger NIA. Accordingly, the stilbene derivative DIDS was found to cause a marked augmentation of the NIA (Fig. 4*A*), which increased from 0.37 ± 0.03 to 0.53 ± 0.03 unit pH ($p < 0.001$, paired *t* test; 14 cells/3 coverslips). When Cl^- was removed from the superfusate, the NIA was similarly increased (Fig. 4*B*) from 0.24 ± 0.01 to 0.34 ± 0.02 unit pH ($p < 0.001$, paired *t* test; 23 cells/3 coverslips).

Sterling et al. (2002) reported that, when AE3 was expressed in HEK293 cells, its transport of bicarbonate was facilitated by the coexpression of surface CA4. If a similar facilitation occurred during the rise of the NIA, then DIDS (by blocking Cl^-–HCO_3^- exchange) would be expected to blunt or completely block the normal effect of benzolamide. Indeed, when benzolamide was applied in the continuous presence of DIDS, it decreased the amplitude of the NIA from 0.51 ± 0.03 to 0.43 ± 0.02 unit pH (Fig. 5*A*) ($p < 0.01$; $n = 19$ cells, 3 coverslips). In the absence of external Cl^-, benzolamide also failed to increase the NIA, which had amplitudes of 0.29 ± 0.01 versus 0.29 ± 0.02 unit pH, before after the addition of the drug, respectively (Fig. 5*B*) ($p = 0.57$; $n = 64$ cells, 3 coverslips).

Surface CA facilitates the Cl^-–HCO_3^- exchanger AE3

In brain, the major Cl^-–HCO_3^- exchanger isoform is AE3, which is abundantly expressed in neurons (Kopito et al., 1989; Raley-Susman et al., 1993; Hentschke et al., 2006). Indeed, real-time PCR measurements on our neuronal cultures showed a fivefold predominance of AE3 over AE2 transcripts (Fig. 6*B*), suggesting that AE3 was in fact the principal Cl^-–HCO_3^- exchanger in these neurons. Transcripts for AE1 were negligible. Single-cell PCR performed on acutely dissociated mouse hippocampal pyramidal neurons indicated abundant transcripts for AE3 in these cells (Fig. 6*A*). Accordingly, one would expect that the effects of benzolamide on neuronal Cl^-–HCO_3^- exchange were related to the facilitation of AE3 by the surface CA.

If the effects of benzolamide were attributable to elimination of surface CA activity that normally served to facilitate AE3, then

the amplification of the NIA by this drug should be eliminated in the absence of this Cl^-–HCO_3^- exchanger. We tested this hypothesis using acutely dissociated, adult, hippocampal pyramidal neurons (from cornu ammon 1) obtained from AE3 knock-out versus wild-type mice. In wild-type neurons, benzolamide caused a typical, significant increase in the NIA amplitude as shown in Figure 7*A* (0.28 ± 0.04 unit pH in control vs 0.39 ± 0.05 unit pH in benzolamide; n = 14 cells, 5 coverslips; $p < 0.01$). In contrast, in neurons from AE3 knock-out mice, benzolamide had no effect on the NIA (Fig. 7*B*) (0.47 ± 0.07 unit pH in control vs 0.45 ± 0.06 unit pH; $n = 7$ cells, 6 coverslips). However, the amplitude of the control NIA was significantly greater in the AE3 knock-out neurons (0.47 ± 0.07 unit pH; $n = 7$ cells, 6 coverslips) compared with wild type (0.28 ± 0.04 unit pH; $n = 14$ cells, 5 coverslips; $p < 0.05$, unpaired t test).

The lack of effect of benzolamide on the NIA in AE3 knock-out neurons might be explained if the surface CAs had been downregulated in the absence of AE3. However, real-time PCR measurements from hippocampus showed increased transcripts for both CA4 and CA14 in the knock-out tissue, although only CA14 message was significantly greater than wild type (Fig. 6*C*). Thus, the absent effect of benzolamide in the AE3-null cells was not attributable to lower expression of these surface enzymes.

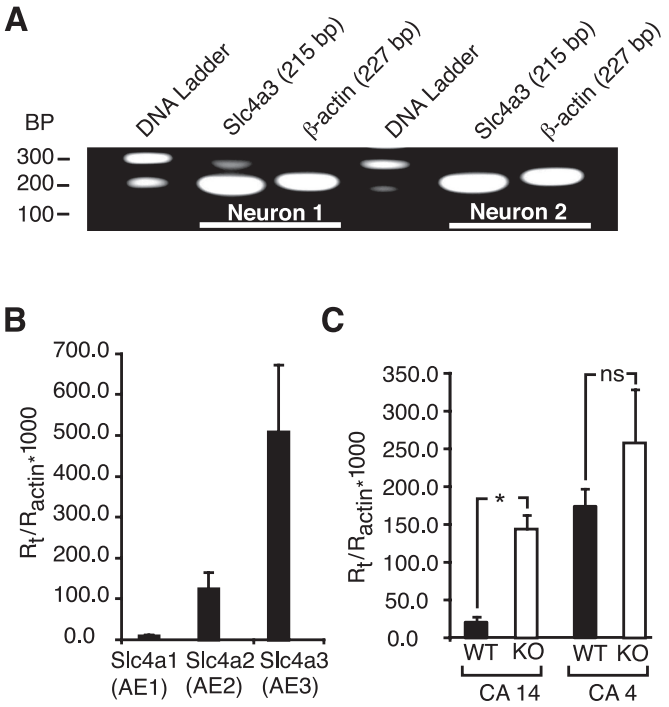

Figure 6. Detection of anion exchanger and ECA transcripts. ***A***, Single-cell (nested) PCR demonstrated abundant AE3 message in individual, acutely dissociated hippocampal pyramidal neurons (area cornu ammon 1). ***B***, Real-time PCR of hippocampal neuronal cultures showed absence of AE1, and an approximately fivefold predominance of AE3 over AE2 transcripts. ***C***, CA14 transcripts were increased in hippocampus from knock-out (KO) mice. There was no significant difference in CA4 transcripts in the same tissues. $^*p < 0.05$; $^{ns}p > 0.05$. Error bars indicate SEM.

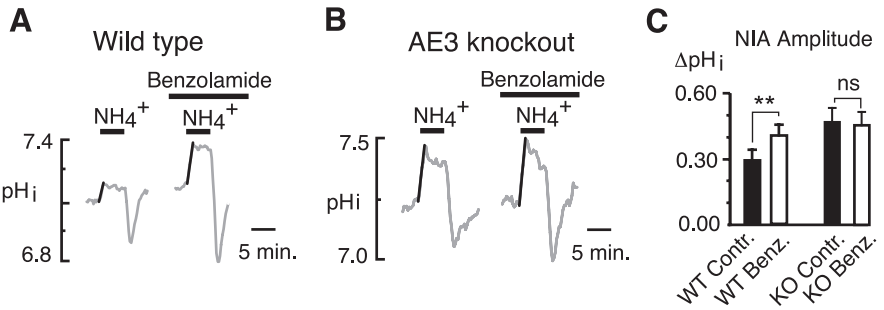

Figure 7. Benzolamide has no effect on the NIA in hippocampal neurons from AE3 knock-out mice. ***A***, Typical amplification of the NIA in a pyramidal neuron acutely dissociated from a wild-type mouse and overall significant increase in the NIA in the 14 neurons studied. ***B***, Similar experiment on a neuron acutely dissociated from the hippocampus of an AE3 knock-out mouse. Benzolamide had no effect on the NIA in this neuron and caused no significant change in the NIA among seven cells studied. Neurons were all obtained from area cornu ammon 1. ***C***, Mean amplitudes of the NIA in wild-type mice controls (WT contr.) versus benzolamide (WT benzolamide), and in knock-out mice controls (KO contr.) versus benzolamide (KO Benz.). $^{**}p < 0.01$; $^{ns}p > 0.05$. Error bars indicate SEM.

Discussion

Brain ECA activity was initially demonstrated in physiological studies that showed the importance of this enzymatic activity in the regulation of activity-dependent alkaline shifts in rat hippocampal slices (Chen and Chesler, 1992a,b; Kaila et al., 1992). Extension of this work to mouse knock-out models demonstrated that CA4 and CA14 can each catalyze the buffering of pH_e transients, and that loss of both enzymes severely disrupts the regulation of extracellular pH (Shah et al., 2005). The present data indicate that ECAs also foster acid loading of neuronal cytosol. The principal finding is that both neuronal CA4 and CA14 augment operation of the Cl^-–HCO_3^- exchanger AE3 in hippocampal neurons, the first such demonstration outside of a heterologous expression system.

The Cl^-–HCO_3^- exchangers function as passive acid loaders, and operate with acid extrusion mechanisms to maintain a stable, steady-state pH_i (Boron, 2004). In response to a rise in pH_i, a passive Cl^-–HCO_3^- exchanger will export bicarbonate and thereby oppose the alkalosis. Thus, in hippocampal neurons, the NIA was increased when Cl^-–HCO_3^- exchange was eliminated by DIDS, zero Cl^- saline, or via the knock-out of AE3. A similar increase in the NIA occurred in the presence of benzolamide, indicating that the extrusion of bicarbonate by AE3 was reliant on the function of surface CA. The action of this drug could be solely attributed to the interaction of AE3 and surface enzyme, because benzolamide had no effect on the NIA in neurons from AE3 knock-out animals. The use of specific inhibitory antibodies demonstrated that both CA4 and CA14 could serve in this role.

Although CAs have long been associated with bicarbonate transport, recent work has emphasized the tight functional coupling between these enzymes and bicarbonate transport proteins (McMurtrie et al., 2004). The facilitation of Cl^-–HCO_3^- exchange by surface CA4 was originally demonstrated in a transfected cell expression system. Sterling et al. (2002) showed that bicarbonate transport by AE1, AE2, or AE3 could be enhanced in HEK293 cells when either of these carriers were coexpressed with CA4. This demonstration required the elimination of intracellular CA activity of the HEK cell (by

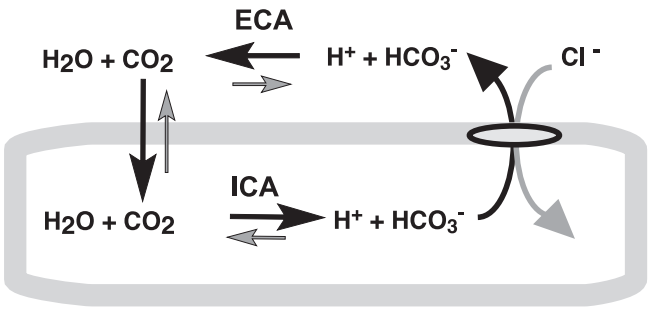

Figure 8. Hypothetical sequence of transmembrane fluxes initiated by an acid-loading Cl^-–HCO_3^- exchanger. The bold arrows display principal fluxes. Maintenance of CO_2 needed to drive intracellular acidification via intracellular carbonic anhydrase (ICA) is dependent on ECA catalyzing the rapid conversion of HCO_3^- and H^+ to CO_2.

overexpression of a dominant-negative CA2), because the internal enzyme alone appeared sufficient to drive maximum AE transport. In hippocampal neurons, in contrast, the facilitation of Cl^-–HCO_3^- exchange by surface CA was robust without manipulation of intracellular CA activity, indicating a less dominant role of cytosolic CA in AE3 function, compared with the heterologous system.

Sterling et al. (2002) suggested that CA4 facilitates AE3-mediated bicarbonate efflux by minimizing the accumulation of bicarbonate on the outer surface membrane. Accordingly, by catalyzing the dehydration of bicarbonate, the enzyme would foster the rapid removal of this anion at the extracellular face of membrane and thereby minimize the backward reaction. Limiting the rise in bicarbonate near the membrane would no doubt aid in its net efflux to some degree; however, it seems unlikely that the buildup of bicarbonate (in the absence of CA4 activity) would amount to a significant proportional change in concentration, given an already high extracellular bicarbonate level of 26 mM. Accordingly, impact of bicarbonate accumulation on the reverse reaction (bicarbonate influx) would be minimal. As such, local bicarbonate removal would not seem the most compelling consequence of ECA activity from the standpoint of AE function.

However, the background concentration of CO_2 is only ~1 mM on both sides of the membrane. Efflux of bicarbonate manifests as a fall in pH_i only as cytosolic CO_2 is hydrated to form H^+. Given a total intracellular buffering capacity of 30 mM, a fall in intracellular pH of 0.1 unit pH would require the bicarbonate to decrease by 3 mM. With a change of this magnitude, depletion of intracellular CO_2 would rapidly ensue if not for the influx of the gas from the microenvironment near the external surface membrane. Although physiologists often assume that CO_2 equilibrates rapidly with an essentially limitless pool, under conditions in which the rate of CO_2 influx is considerable, the external surface can in fact become very alkaline because of depletion of the gas from the local microenvironment (Vanheel et al., 1986). This may be a considerable factor for neurons and glia, which can have a highly folded surface membrane. Surface CA would therefore serve to rapidly replenish the extracellular CO_2 in the external microenvironment, and thereby avoid a shortfall in the intracellular CO_2 that is required to generate the AE3-mediated fall in pH_i (Fig. 8). In essence, the surface enzyme would serve to recycle the extruded bicarbonate as local CO_2. Thus, avoidance of CO_2 depletion adjacent to the plasma membrane would seem to be a plausible basis by which ECA facilitates the function of chloride–bicarbonate exchangers.

The CA4 isoform is entirely extracellular, tethered to the surface membrane by a phosphatidylinositol glycan linkage (Zhu and Sly, 1990; Waheed et al., 1992b). However, CA14 is a transmembrane protein with an extracellular catalytic domain. The facilitation of Cl^-–HCO_3^- exchange by CA14 complements the previous demonstration of a functional interaction of AE3 with another transmembrane CA isoform. CA9 is a transmembrane protein with an extracellular catalytic domain, recently shown to facilitate bicarbonate transport by AE3 (Morgan et al., 2007). Coimmunoprecipitation studies have shown that AE3 can pull down CA4 (Sterling et al., 2002) and CA9 (Morgan et al., 2007), suggesting that the facilitation of Cl^-–HCO_3^- exchange could be enhanced by a structural association that might occur via direct molecular interaction. Preliminary pull-down studies have also suggested some structural association between CA14 and AE3 (Casey, 2007).

It is noteworthy that the endogenous intracellular CA2 of HEK293 cells has been reported to augment Cl^-–HCO_3^- exchange by SLC26A7 without directly binding to the transporter (Morgan et al., 2007). Thus, simple proximity of a freely diffusible CA may be sufficient to facilitate bicarbonate transport. If ECA isoforms function to replenish surface CO_2 during the AE3-mediated efflux of HCO_3^-, and thereby preserve the drive for intracellular acidification, it is plausible this might be accomplished without a direct molecular interaction with the transporter.

The predominance of AE3 in brain suggests a prominent role in acid–base balance in the nervous system. AE3-null mice have been shown to have a reduced seizure threshold (Hentschke et al., 2006) and degeneration of photoreceptors leading to blindness (Yang et al., 2005). Functional retinal defects have been demonstrated in CA14-null mice, and this dysfunction became far worse with concomitant knock-out of CA4 (Ogilvie et al., 2007). The specific deficits in pH regulation that underlie these multiple pathologies are not known. Large increases in pH_i of neurons, as induced experimentally here, are not commonly encountered. In fact, neural activity typically results in a fall in pH_i, secondary to the entry of Ca^{2+} ions (Chesler, 2003). Nonetheless, maintenance of steady-state pH_i of hippocampal pyramidal neurons is likely to entail concomitant acid extrusion and acid loading (Brett et al., 2002). The inability to effectively acid load may therefore result in excessively high steady-state pH_i that leads to particular deficits in susceptible populations of neurons.

The functional relationship between ECA and AE3 may also contribute to the reversal potential of fast inhibitory synaptic potentials. In early development, IPSPs are depolarizing, because of the inward transport of Cl^- (Farrant and Kaila, 2007). Embryonic motoneurons appear to accomplish Cl^- loading using both the Na^+–K^+–$2Cl^-$ transporter NKCC1, and AE3 (Gonzalez-Islas et al., 2008). Later in development, IPSPs become hyperpolarizing because of the expression of the outward K^+–Cl^- cotransporter KCC2 (Rivera et al., 1999). In some mature neurons, however, the reversal potential for $GABA_A$-mediated IPSPs is not homogenous across the cell, and can be more depolarized in discrete regions such as the axon initial segment (Szabadics et al., 2006). This heterogeneity appears linked to the membrane distribution of NKCC1 versus KCC2 (Khirug et al., 2008). The local tonic activity of AE3 is likely to also contribute to the net balance of intracellular Cl^-. Brett et al. (2002) noted apparent tonic Cl^-–HCO_3^- exchanger activity in the subset of acutely dissociated hippocampal (cornu ammon 1) neurons with higher baseline pH_i. Thus, the degree of AE3 activity at a given pH_i is likely to contribute to the steady-state cytosolic Cl^- load of neurons and may thereby influence fast GABAergic and glycinergic inhibitory synaptic transmission.

References

Alvarez BV, Loiselle FB, Supuran CT, Schwartz GJ, Casey JR (2003) Direct extracellular interaction between carbonic anhydrase IV and the human NBC1 sodium/bicarbonate co-transporter. Biochemistry 42:12321–12329.

Boron WF (2004) Regulation of intracellular pH. Adv Physiol Educ 28:160–179.

Boron WF, De Weer P (1976) Intracellular pH transients in squid giant axons caused by CO_2, NH_3, and metabolic inhibitors. J Gen Physiol 67:91–112.

Boyarsky G, Ganz MB, Sterzel RB, Boron WF (1988) pH regulation in single glomerular mesangial cells. I. Acid extrusion in absence and presence of HCO_3. Am J Physiol 255:C844–C856.

Breton S (2001) The cellular physiology of carbonic anhydrases. JOP 2:159–164.

Brett CL, Kelly T, Sheldon C, Church J (2002) Regulation of Cl^--HCO_3^- exchangers by cAMP-dependent protein kinase in adult rat hippocampal CA1 neurons. J Physiol 545:837–853.

Casey J (2007) Physical and functional complex of AE3 Cl^-/HCO_3^- exchanger and carbonic anhydrase XIV in the inner retina and brain. Paper presented at the Association for Research in Vision and Ophthalmology Annual Meeting, Fort Lauderdale, FL, May.

Chen JC, Chesler M (1992a) Modulation of extracellular pH by glutamate and GABA in rat hippocampal slices. J Neurophysiol 67:29–36.

Chen JC, Chesler M (1992b) pH transients evoked by excitatory synaptic transmission are increased by inhibition of extracellular carbonic anhydrase. Proc Natl Acad Sci U S A 89:7786–7790.

Chesler M (2003) Regulation and modulation of pH in the brain. Physiol Rev 83:1183–1221.

Farrant M, Kaila K (2007) The cellular, molecular and ionic basis of GABAA receptor signalling. Prog Brain Res 160:59–87.

Fedirko N, Avshalumov M, Rice ME, Chesler M (2007) Regulation of postsynaptic Ca^{2+} influx in hippocampal CA1 pyramidal neurons via extracellular carbonic anhydrase. J Neurosci 27:1167–1175.

Gonzalez-Islas C, Chub N, Wenner P (2008) NKCC1 and AE3 appear to accumulate chloride in embryonic motoneurons. J Neurophysiol 101:507–518.

Hentschke M, Wiemann M, Hentschke S, Kurth I, Hermans-Borgmeyer I, Seidenbecher T, Jentsch TJ, Gal A, Hübner CA (2006) Mice with a targeted disruption of the Cl^-/HCO_3^- exchanger AE3 display a reduced seizure threshold. Mol Cell Biol 26:182–191.

Kaila K, Paalasmaa P, Taira T, Voipio J (1992) pH transients due to monosynaptic activation of GABAA receptors in rat hippocampal slices. Neuroreport 3:105–108.

Kaunisto K, Parkkila S, Rajaniemi H, Waheed A, Grubb J, Sly WS (2002) Carbonic anhydrase XIV: luminal expression suggests key role in renal acidification. Kidney Int 61:2111–2118.

Khirug S, Yamada J, Afzalov R, Voipio J, Khiroug L, Kaila K (2008) GABAergic depolarization of the axon initial segment in cortical principal neurons is caused by the Na–K–2Cl cotransporter NKCC1. J Neurosci 28:4635–4639.

Kopito RR, Lee BS, Simmons DM, Lindsey AE, Morgans CW, Schneider K (1989) Regulation of intracellular pH by a neuronal homolog of the erythrocyte anion exchanger. Cell 59:927–937.

Liu W, Saint DA (2002) Validation of a quantitative method for real time PCR kinetics. Biochem Biophys Res Commun 294:347–353.

Maren TH (1960) A simplified micromethod for the determination of carbonic anhydrase and its inhibitors. J Pharmacol Exp Ther 130:26–29.

McMurtrie HL, Cleary HJ, Alvarez BV, Loiselle FB, Sterling D, Morgan PE, Johnson DE, Casey JR (2004) The bicarbonate transport metabolon. J Enzyme Inhib Med Chem 19:231–236.

Mintz IM, Adams ME, Bean BP (1992) P-type calcium channels in rat central and peripheral neurons. Neuron 9:85–95.

Morgan PE, Pastoreková S, Stuart-Tilley AK, Alper SL, Casey JR (2007) Interactions of transmembrane carbonic anhydrase, CAIX, with bicarbonate transporters. Am J Physiol Cell Physiol 293:C738–C748.

Ogilvie JM, Ohlemiller KK, Shah GN, Ulmasov B, Becker TA, Waheed A, Hennig AK, Lukasiewicz PD, Sly WS (2007) Carbonic anhydrase XIV deficiency produces a functional defect in the retinal light response. Proc Natl Acad Sci U S A 104:8514–8519.

Parkkila S, Parkkila AK, Rajaniemi H, Shah GN, Grubb JH, Waheed A, Sly WS (2001) Expression of membrane-associated carbonic anhydrase XIV on neurons and axons in mouse and human brain. Proc Natl Acad Sci U S A 98:1918–1923.

Raley-Susman KM, Sapolsky RM, Kopito RR (1993) Cl^-/HCO_3^- exchange functions differs in adult and fetal rat hippocampal neurons. Brain Res 614:308–314.

Rivera C, Voipio J, Payne JA, Ruusuvuori E, Lahtinen H, Lamsa K, Pirvola U, Saarma M, Kaila K (1999) (1999) The K^+-Cl^- co-transporter KCC2 renders GABA hyperpolarizing during neuronal maturation. Nature 397:251–255.

Romero MF, Fulton CM, Boron WF (2004) The SLC4 family of HCO_3^- transporters. Pflugers Arch 447:495–509.

Roos A, Boron WF (1981) Intracellular pH. Physiol Rev 61:296–433.

Shah GN, Ulmasov B, Waheed A, Becker T, Makani S, Svichar N, Chesler M, Sly WS (2005) Carbonic anhydrase IV and XIV knockout mice: roles of the respective carbonic anhydrases in buffering the extracellular space in brain. Proc Natl Acad Sci U S A 102:16771–16776.

Sterling D, Alvarez BV, Casey JR (2002) The extracellular component of a transport metabolon. Extracellular loop 4 of the human AE1 Cl^-/HCO_3^- exchanger binds carbonic anhydrase IV. J Biol Chem 277:25239–25246.

Sundaram V, Rumbolo P, Grubb J, Strisciuglio P, Sly WS (1986) Carbonic anhydrase II deficiency: diagnosis and carrier detection using differential enzyme inhibition and inactivation. Am J Hum Genet 38:125–136.

Svichar N, Waheed A, WS Sly, Hennings JC, Hubner C, Chesler M (2007) Functional link between surface carbonic anhydrases and chloride-bicarbonate exchange in neurons and astrocytes. Soc Neurosci Abstr 33:683.17.

Szabadics J, Varga C, Molnár G, Oláh S, Barzó P, Tamás G (2006) Excitatory effect of GABAergic axo-axonic cells in cortical microcircuits. Science 311:233–235.

Thomas RC (1984) Experimental displacement of intracellular pH and the mechanism of its subsequent recovery. J Physiol 354:3P–22P.

Tong CK, Brion LP, Suarez C, Chesler M (2000) Interstitial carbonic anhydrase (CA) activity in brain is attributable to membrane-bound CA type IV. J Neurosci 20:8247–8253.

Tse FW, Fraser DD, Duffy S, MacVicar BA (1992) Voltage-activated K^+ currents in acutely isolated hippocampal astrocytes. J Neurosci 12:1781–1788.

Vanheel B, De Hemptinne A, Leusen I (1986) Influence of surface pH on intracellular pH regulation in cardiac skeletal muscle. Am J Physiol 250:C748–C760.

Waheed A, Zhu XL, Sly WS (1992a) Membrane-associated carbonic anhydrase from rat lung. Purification, characterization, tissue distribution, and comparison with carbonic anhydrase IVs of other mammals. J Biol Chem 267:3308–3311.

Waheed A, Zhu XL, Sly WS, Wetzel P, Gros G (1992b) Rat skeletal muscle membrane associated carbonic anhydrase is 39-kDa glycosylated GPI-anchored CA IV. Arch Biochem Biophys 294:550–556.

Wang W, Bradley SR, Richerson GB (2002) Quantification of the response of rat medullary raphe neurones to independent changes in pH(o) and $P(CO_2)$. J Physiol 540:951–970.

Wistrand PJ, Knuuttila KG (1989) Renal membrane-bound carbonic anhydrase. Purification and properties. Kidney Int 35:851–859.

Wu Q, Pierce WM Jr, Delamere NA (1998) Cytoplasmic pH responses to carbonic anhydrase inhibitors in cultured rabbit nonpigmented ciliary epithelium. J Membr Biol 162:31–38.

Yang Z, Alvarez BV, Chakarova C, Jiang L, Karan G, Frederick JM, Zhao Y, Sauvé Y, Li X, Zrenner E, Wissinger B, Hollander AI, Katz B, Baehr W, Cremers FP, Casey JR, Bhattacharya SS, Zhang K (2005) Mutant carbonic anhydrase 4 impairs pH regulation and causes retinal photoreceptor degeneration. Hum Mol Genet 14:255–265.

Zhu XL, Sly WS (1990) Carbonic anhydrase IV from human lung. Purification, characterization, and comparison with membrane carbonic anhydrase from human kidney. J Biol Chem 265:8795–8801.